Hindawi
Mathematical Problems in Engineering
Volume 2022, Article ID 1947098, 9 pages
https://doi.org/10.1155/2022/1947098

Research Article

A New Generalized Modified Weibull Model: Simulating and Modeling the Dynamics of the COVID-19 Pandemic in Saudi Arabia and Egypt

Walid Emam and Yusra Tashkandy

Department of Statistics and Operations Research, Faculty of Science, King Saud University, P.O. Box 2455, Riyadh 11451, Saudi Arabia

Correspondence should be addressed to Walid Emam; walid_emam42@yahoo.com

Received 6 January 2022; Accepted 12 March 2022; Published 21 April 2022

Academic Editor: Massimiliano Ferrara

The flare-up of coronavirus disease 2019 (COVID-19) was first identified in China and then spread worldwide. The concerning articles are significant because of their increasing average infection rate. The exact scientific anatomy of this circumstance remains to be discussed. Nevertheless, it is important for governments and all responsible organizations to have sound statistics and analysis to decide on possible necessary actions. This article compares the dynamics of the COVID-19 pandemic between Saudi Arabia and Egypt. We provide an appropriate process of convergence of facts that can be useful for both administrations to implement appropriate quarantine procedures. In addition, the new generalized modified Weibull distribution is provided to provide the preferred description about COVID-19 total cases, daily new cases, total deaths, and daily death statistics of Saudi Arabia and Egypt.

1. Introduction

This article has the potential to compare the COVID-19 pandemic outbreak in Saudi Arabia and Egypt. We present a new flexible model to represent the COVID-19 pandemic and closely examine its behavior. The extended model is an improvement of COVID-19 modeling. We refer to some comparisons of epidemic dynamics between different countries in [1–14]. Figure 1 shows the latest information on the total number of COVID-19 cases in Saudi Arabia 1(a) and Egypt 1(b). Figure 2 shows the daily new cases in Saudi Arabia 2(a) and Egypt 2(b).

Figure 3 shows the total number of COVID-19 deaths in Saudi Arabia 3(a) and Egypt 3(b). Figure 4 shows daily COVID-19 deaths in Saudi Arabia 4(a) and Egypt 4(b). The gamma, exponential, and Weibull distributions are poor models for fitting the defensible data. Defensible data require the use of a model that is sufficiently fitted within its framework (see Dutta and Perry [15]). Many researchers have adopted new families of distributions (see Ahmad et al. [16], Ahmad et al. [17], Nasir et al. [18], Jamal and Nasir [19], Al-Mofleh [20], Afify et al. [21], Afify and Alizadeh [22], and Cordeiro et al. [23]). In this article, the new method of generalized U-family is used to propose an extended class of statistical models. Suppose $W(u;\Xi)$ is the CDF and $w(u;\varphi)$ is the PDF of an R.V. The CDF $\mathrm{F}(u;\rho,\Xi)$ of the new generalized-U (NG -U) family of distributions (see Alzaatreh [24]), is given by

$$|(u;\rho,\Xi) = 1 - \left(\frac{\left[1 - W(u;\Xi)^2\right]^{\rho}}{\exp\left[W(u;\Xi)^2\right]}\right), \quad \rho > 0, u \in \mathbb{R}, \qquad (1)$$

where Ξ is the parameter vector. The corresponding PDF, survival function (SF), and hazard rate function (HRF) of R.V.X over the NG-U family are given, respectively, as

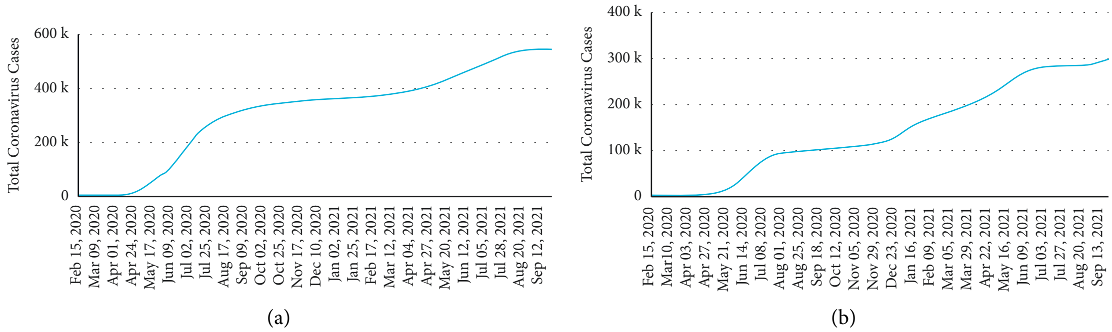

Figure 1: Plots for total COVID-19 cases in Saudi Arabia (a) and Egypt (b).

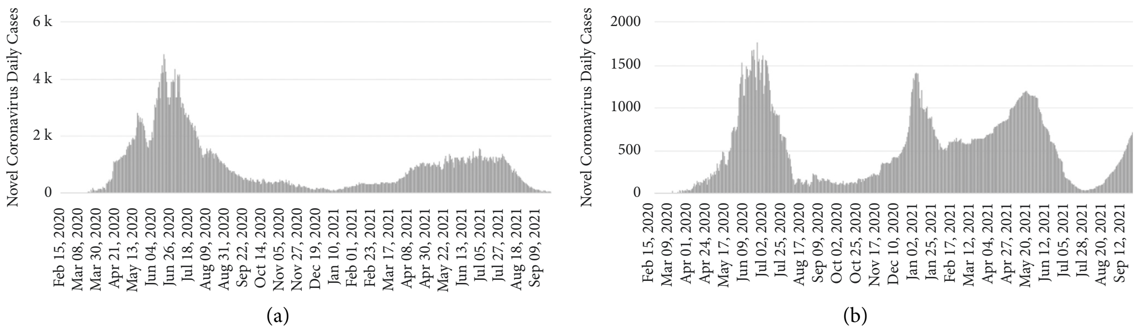

Figure 2: Plots for daily new cases in Saudi Arabia (a) and Egypt (b).

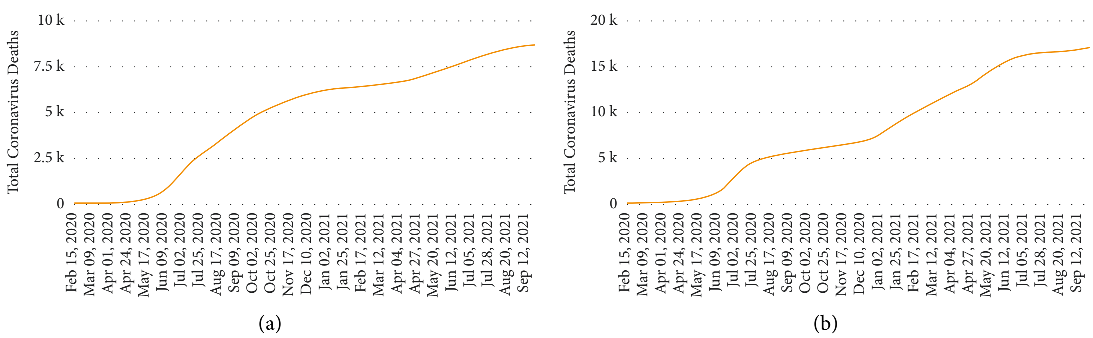

Figure 3: Plots for total COVID-19 deaths in Saudi Arabia (a) and Egypt (b).

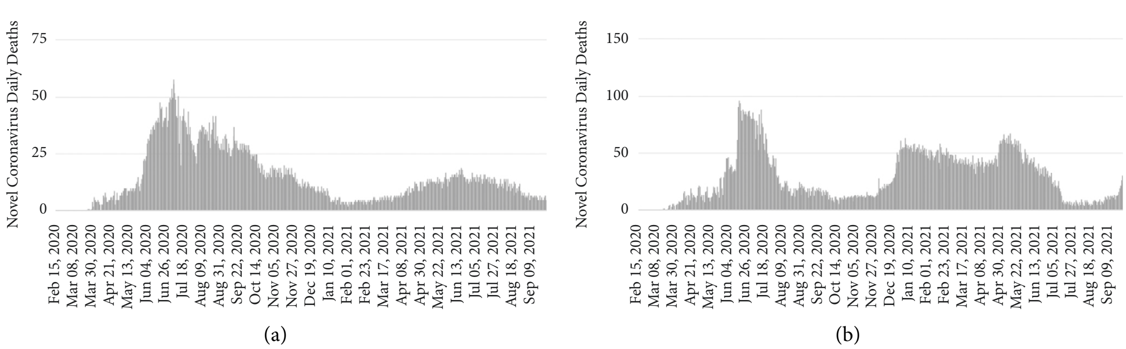

Figure 4: Plots for daily deaths in Saudi Arabia (a) and Egypt (b).

$$f(u;\rho,\Xi)=2e^{-W(u;\Xi)^2}w(u;\Xi)W(u;\Xi)\left(1-W(u;\Xi)^2\right)^{\rho-1}\left(1-W(u;\Xi)^2+\rho\right),$$
$$S(u;\rho,\Xi)=e^{-W(u;\Xi)^2}\left(1-W(u;\Xi)^2\right)^{\rho}, \quad (2)$$
$$h(u;\rho,\Xi)=2w(u;\Xi)W(u;\Xi)\left(1-W(u;\Xi)^2\right)^{-1}\left(1-W(u;\Xi)^2+\rho\right).$$

With the new CDF of NG-U, many new flexible models with heavy tails can be obtained. Based on the NG-U approach, some newly added models are presented in Table 1. This article is organized as follows: Section 2 defines the new generalized modified Weibull distribution (NG-MW). Section 3 provides the maximum likelihood estimators (MLEs). Section 4 provides the Bayesian estimators. Section 5 performs a simulation discussion. Section 6 analyzes COVID-19 real data to illustrate its potential. Section 7 provides concluding remarks.

2. Submodel Description

The modified Weibull distribution is one of the most memorable modifications of the Weibull distribution, developed to provide adaptability to the exponential, Rayleigh, linear failure rate, and Weibull distributions (see [25]). We further develop this area of distribution theory and provide a new memorable version of the modified Weibull model to improve its adaptability. The modified Weibull distribution with three parameters $\Xi=(\delta,\eta,\zeta)$ has CDF, PDF, SF, and HRF and is given by

$$W(x;\delta,\eta,\zeta)=1-e^{-\delta x-\eta x^{\zeta}}, \quad x>0,\ \zeta>0,\delta,\ \eta\geq 0,\ \xi+\eta>0,$$
$$w(x;\delta,\eta,\zeta)=e^{-\delta x-\eta x^{\zeta}}\left(\delta+x^{\zeta-1}\eta\zeta\right), \quad x>0,\ \zeta>0,\delta,\ \eta\geq 0,\ \delta+\eta>0,$$
$$S(x;\delta,\eta,\zeta)=e^{-\delta x-\eta x^{\zeta}}, \quad x>0,\ \zeta>0,\delta,\ \eta\geq 0,\ \delta+\eta>0, \quad (3)$$
$$h(x;\delta,\eta,\zeta)=\delta+\eta\zeta x^{\zeta-1}, \quad x>0,\ \zeta>0,\delta,\ \eta\geq 0,\ \delta+\eta>0.$$

We introduce the NG-MW distribution and examine the setting of its PDF, SF, and HRF. An R.V.X follows the NG-MW distribution if its CDF takes the form

$$F(x;\delta,\eta,\zeta,\rho)=1-e^{-\left(1-e^{-x\delta-x^{\zeta}\eta}\right)^2}\left(1-\left(1-e^{-x\delta-x^{\zeta}\eta}\right)^2\right)^{\rho}. \quad (4)$$

where $x>0,\zeta,\rho>0,\delta,\eta\geq 0$, and $\delta+\eta>0$. The PDF, SF, and HRF of the NG-MW distribution are, respectively, given by

$$f(x;\delta,\eta,\zeta,\rho)=2e^{-\delta x-\eta x^{\zeta}-\left(-1+e^{-\delta x-\eta x^{\zeta}}\right)^2}\left(\delta+\eta\zeta x^{\zeta-1}\right)\left(1-e^{-\delta x-\eta x^{\zeta}}\right)$$
$$\times\left(1-\left(-1+e^{-x\delta-x^{\zeta}\eta}\right)^2\right)^{\rho-1}\left(1-\left(-1+e^{-x\delta-x^{\zeta}\eta}\right)^2+\rho\right), \quad (5)$$
$$S(x;\delta,\eta,\zeta,\rho)=e^{-\left(1-e^{-x\delta-x^{\zeta}\eta}\right)^2}\left(1-\left(1-e^{-x\delta-x^{\zeta}\eta}\right)^2\right)^{\rho},$$

$$h(x;\delta,\eta,\zeta,\rho)=\frac{2e^{-x\delta-x^{\zeta}\eta}\left(\delta+x^{-1+\zeta}\eta\zeta\right)\left(1-e^{-x\delta-x^{\zeta}\eta}\right)\left(1-\left(1-e^{-x\delta-x^{\zeta}\eta}\right)^2+\rho\right)}{1-\left(1-e^{-x\delta-x^{\zeta}\eta}\right)^2}. \quad (6)$$

Table 1: New submodules via the NG-X family.

No.	Model	Survival function	Generated model
1	Beta	$([1-I_x(a,b)^2]^{\rho}/\exp[I_x(a,b)^2])$	$a, b, \rho>0$
2	Burr	$([1-1-(1+x^a)^{-2b}]^{\rho}/\exp[1-(1+x^a)^{-2b}])$	$a, b, \rho>0$
3	Erlang	$([1-((1/(a-1)!))\gamma(a,bx)^2]^{\rho}/\exp[((1/(a-1)!))\gamma(a,bx)])$	$a, b, \rho>0$
4	Exponential	$([1-1-\exp(-ax)^2]^{\rho}/\exp[1-\exp(-ax)^2])$	$a, \rho>0$
5	Frechet	$([1-\exp(-(x/b)^{-a})^2]^{\rho}/\exp[\exp(-(x/b)^{-a})^2])$	$a, b, \rho>0$
6	Gamma	$([1-\gamma(a,bx)\gamma(a)^2]^{\rho}/\exp[\gamma(a,bx)\gamma(a)^2])$	$a, b, \rho>0$
7	Gumbel	$([1-\exp(-\exp(-(x-a)/b))^2]^{\rho}/\exp[\exp(-\exp(-(x-a)/b))^2])$	$b, \rho>0$
8	Half logistic	$([1-(1-\exp(-x))/(1+\exp(-x))^2]^{\rho}/\exp[(1-\exp(-x))/(1+\exp(-x))^2])$	$\rho>0$
9	Kumaraswamy	$([1-1-(1-x^a)^2 b]^{\rho}/\exp[1-(1-x^a)^2 b])$	$a, b, \rho>0$
10	Lindely	$([1-1-((\exp(-ax)(1+a+ax))/(1+a))^2]^{\rho}/\exp[1-((\exp(-ax)(1+a+ax))/(1+a))^2])$	$a, \rho>0$
11	Linear failure rate	$([1-1-\exp(-ax^b-cx)^2]^{\rho}/\exp[1-\exp(-ax^b-cx)^2])$	$a, b, c, \rho>0$
12	Log logistics	$[1-(1/(1+(x/b)^{-a}))^2]^{\rho}/\exp[(1/(1+(x/b)^{-a}))]$	$a, b, \rho>0$
13	Lomax	$[1-1-(1+ax)^{-2b}]^{\rho}/\exp[1-(1+ax)^{-2b}]$	$a, b, \rho>0$
14	Normal	$([1-\phi((x-a)/b)^2]^{\rho}/\exp[\phi((x-a)/b)^2])$	$b, \rho>0$
15	Pareto	$[1-1-(x_m/x)^2 a]^{\rho}/\exp[1-(x_m/x)^2 a]$	$a, x_m, \rho>0$
16	Power function	$([1-(x/b)^2 a]^{\rho}/\exp[(x/b)^2 a])$	$a, b, \rho>0$
17	Rayleigh	$[1-1-\exp(-ax^2)^2]^{\rho}/\exp[1-\exp(-ax^2)^2]$	$a, \rho>0$
18	Topp Leone	$([1-x^a(2-x^a)^2]^{\rho}/\exp[x^a(2-x^a)^2])$	$a, b, \rho>0$
19	Uniform	$([1-(x/a)^2]^{\rho}/\exp[(x/a)^2])$	$a, \rho>0$
20	Weibull	$([1-1-\exp(-ax^b)^2]^{\rho}/\exp[1-\exp(-ax^b)^2])$	$a, b, \rho>0$

The model NG-MW reduces to the NG-Weibull distribution when $\delta=1$, and reduces to the modified Weibull distribution when $\rho=1$.

3. Maximum Likelihood Estimation

Let the observed values $x_1, x_2, \ldots, x_n$ of $X_1, X_2, \ldots, X_n$ be a random sample from the model NG-X. The NG-X probability is

$$l = 2^n e^{-\sum_{i=1}^{n} W(x_i;\Xi)^2} \prod_{i=1}^{n}\Big(w(x_i;\Xi)W(x_i;\Xi)\big(1-W(x_i;\Xi)^2\big)^{\rho-1}\big(1-W(x_i;\Xi)^2+\rho\big)\Big). \tag{7}$$

The corresponding NG-X log-likelihood is given by

$$\begin{aligned} L = {} & n\mathrm{Log}[2]-\sum_{i=1}^{n} W(x_i;\Xi)^2+\sum_{i=1}^{n}\mathrm{Log}[w(x_i;\Xi)]+\sum_{i=1}^{n}\mathrm{Log}[W(x_i;\Xi)] \\ & +(\rho-1)\sum_{i=1}^{n}\mathrm{Log}\big[1-W(x_i;\Xi)^2\big]+\sum_{i=1}^{n}\mathrm{Log}\big[1+\rho-W(x_i;\Xi)^2\big]. \end{aligned} \tag{8}$$

MLE can be derived by maximizing equation (8) as follows:

$$\frac{\partial L}{\partial \rho}=\sum_{i=1}^{n}\mathrm{Log}\big[1-W(x_i;\Xi)^2\big]+\sum_{i=1}^{n}\frac{1}{1+\rho-W(x_i;\Xi)^2}. \tag{9}$$

Then the NG-MW log-likelihood function has the form

$$
\begin{aligned}
L = n\mathrm{Log}[2] - \sum_{i=1}^{n}\left(1-e^{-\delta x_i-\eta x_i^{\zeta}}\right)^2 + \sum_{i=1}^{n}\mathrm{Log}\left[e^{-x_i\delta-x_i^{\zeta}\eta}\left(\delta+x_i^{\zeta-1}\eta\zeta\right)\right] \\
+\sum_{i=1}^{n}\mathrm{Log}\left[\left(1-e^{-\delta x_i-\eta x_i^{\zeta}}\right)\right] + (\rho-1)\sum_{i=1}^{n}\mathrm{Log}\left[1-\left(1-e^{-\delta x_i-\eta x_i^{\zeta}}\right)^2\right] \\
+\sum_{i=1}^{n}\mathrm{Log}\left[1+\rho-\left(1-e^{-\delta x_i-\eta x_i^{\zeta}}\right)^2\right].
\end{aligned}
\tag{10}
$$

Maximizing equation (10) to obtain the MLE estimates as follows:

$$
\begin{aligned}
\frac{\partial L}{\partial \delta} = \sum_{i=1}^{n}\frac{x_i}{e^{\delta x_i+\eta x_i^{\zeta}}-1} + 2(\rho-1)\sum_{i=1}^{n}\frac{x_i e^{-\delta x_i-\eta x_i^{\zeta}}\left(e^{-\delta x_i-\eta x_i^{\zeta}}-1\right)}{1-\left(1-e^{-\delta x_i-\eta x_i^{\zeta}}\right)^2} \\
+2\sum_{i=1}^{n}\left(\frac{1}{1+\rho-\left(1-e^{-\delta x_i-\eta x_i^{\zeta}}\right)^2}+1\right)x_i e^{-\delta x_i-\eta x_i^{\zeta}}\left(e^{-\delta x_i-\eta x_i^{\zeta}}-1\right) \\
+\sum_{i=1}^{n}\frac{1-x_i\left(\delta+\eta\zeta x_i^{\zeta-1}\right)}{\delta+\eta\zeta x_i^{\zeta-1}},
\end{aligned}
\tag{11}
$$

$$
\begin{aligned}
\frac{\partial L}{\partial \eta} = \sum_{i=1}^{n}\frac{x_i^{\zeta}}{e^{\delta x_i+\eta x_i^{\zeta}}-1} + 2(\rho-1)\sum_{i=1}^{n}\frac{x_i^{\zeta} e^{-\delta x_i-\eta x_i^{\zeta}}\left(e^{-\delta x_i-\eta x_i^{\zeta}}-1\right)}{1-\left(1-e^{-\delta x_i-\eta x_i^{\zeta}}\right)^2} \\
+2\sum_{i=1}^{n}\left(\frac{1}{1+\rho-\left(1-e^{-\delta x_i-\eta x_i^{\zeta}}\right)^2}+1\right)x_i^{\zeta} e^{-\delta x_i-\eta x_i^{\zeta}}\left(e^{-\delta x_i-\eta x_i^{\zeta}}-1\right) \\
+\sum_{i=1}^{n}\frac{x_i^{\zeta-1}\left(\zeta-x_i\left(\delta+\eta\zeta x_i^{\zeta-1}\right)\right)}{\delta+\eta\zeta x_i^{\zeta-1}},
\end{aligned}
\tag{12}
$$

$$
\begin{aligned}
\frac{\partial L}{\partial \zeta} = \sum_{i=1}^{n}\frac{\eta x_i^{\zeta}\mathrm{Log}[x_i]}{e^{\delta x_i+\eta x_i^{\zeta}}-1} \\
+2\eta(\rho-1)\sum_{i=1}^{n}\frac{\left(e^{-\delta x_i-\eta x_i^{\zeta}}-1\right)x_i^{\zeta}e^{-\delta x_i-\eta x_i^{\zeta}}\mathrm{Log}[x_i]}{1-\left(1-e^{-\delta x_i-\eta x_i^{\zeta}}\right)^2} \\
+2\eta\sum_{i=1}^{n}\frac{\left(e^{-\delta x_i-\eta x_i^{\zeta}}-1\right)x_i^{\zeta}e^{-\delta x_i-\eta x_i^{\zeta}}\mathrm{Log}[x_i]}{1+\rho-\left(1-e^{-\delta x_i-\eta x_i^{\zeta}}\right)^2} \\
+2\eta\sum_{i=1}^{n}\left(e^{-\delta x_i-\eta x_i^{\zeta}}-1\right)x_i^{\zeta}e^{-\delta x_i-\eta x_i^{\zeta}}\mathrm{Log}[x_i] \\
+\sum_{i=1}^{n}\frac{-\eta\mathrm{Log}[x_i]x_i^{\zeta}\left(\delta+\eta\zeta x_i^{\zeta-1}\right)+\left(\eta x_i^{\zeta-1}+\eta\zeta\mathrm{Log}[x_i]x_i^{\zeta-1}\right)}{\delta+\eta\zeta x_i^{\zeta-1}},
\end{aligned}
\tag{13}
$$

$$
\frac{\partial L}{\partial \rho} = \sum_{i=1}^{n}\frac{1}{1+\rho-\left(1-e^{-\delta x_i-\eta x_i^{\zeta}}\right)^2} + \sum_{i=1}^{n}\mathrm{Log}\left[1-\left(1-e^{-\delta x_i-\eta x_i^{\zeta}}\right)^2\right].
\tag{14}
$$

The maximum likelihood estimators of the NG-MW distribution parameters δ, η, ζ, and ρ are the solutions of the above nonlinear equations. Since the equations expressed in (11)–(14) cannot be solved analytically, one must use a numerical procedure to solve them. The asymptotic C.Is of δ, η, ζ, and ρ can be calculated. The variance-covariance matrix $V(\widehat{\kappa}, \widehat{\eta}, \widehat{\zeta}, \widehat{\rho})$ was given by

$$V(\widehat{\kappa}, \widehat{\eta}, \widehat{\zeta}, \widehat{\rho}) = -\begin{bmatrix} \dfrac{\partial^2 L}{\partial \delta^2} & \dfrac{\partial^2 L}{\partial \delta\, \partial \eta} & \dfrac{\partial^2 L}{\partial \delta\, \partial \zeta} & \dfrac{\partial^2 L}{\partial \delta\, \partial \rho} \\ \dfrac{\partial^2 L}{\partial \eta\, \partial \delta} & \dfrac{\partial^2 L}{\partial \eta^2} & \dfrac{\partial^2 L}{\partial \eta\, \partial \zeta} & \dfrac{\partial^2 L}{\partial \eta\, \partial \rho} \\ \dfrac{\partial^2 L}{\partial \zeta\, \partial \delta} & \dfrac{\partial^2 L}{\partial \zeta\, \partial \eta} & \dfrac{\partial^2 L}{\partial \zeta^2} & \dfrac{\partial^2 L}{\partial \zeta\, \partial \rho} \\ \dfrac{\partial^2 L}{\partial \rho\, \partial \delta} & \dfrac{\partial^2 L}{\partial \rho\, \partial \eta} & \dfrac{\partial^2 L}{\partial \rho\, \partial \zeta} & \dfrac{\partial^2 L}{\partial \rho^2} \end{bmatrix}^{-1}. \quad (15)$$

A $100(1-\varepsilon)\%$ two-sided approximate C.Is for δ, η, ζ, and ρ are, respectively, given by

$$\begin{aligned} &\widehat{\delta} \pm z_{(\delta/2)} \sqrt{V(\widehat{\delta})}, \\ &\widehat{\eta} \pm z_{(\delta/2)} \sqrt{V(\widehat{\eta})}, \\ &\widehat{\zeta} \pm z_{(\delta/2)} \sqrt{V(\widehat{\zeta})}, \\ &\widehat{\rho} \pm z_{(\delta/2)} \sqrt{V(\widehat{\rho})}, \end{aligned} \quad (16)$$

where $V(\widehat{\delta}), V(\widehat{\eta}), V(\widehat{\zeta})$, and $V(\widehat{\rho})$ are given by the diagonal elements of $V(\widehat{\delta}, \widehat{\eta}, \widehat{\zeta}, \widehat{\rho})$, and $z_{(\varepsilon/2)}$ is the upper $(\varepsilon/2)$ percentile of the standard normal distribution.

4. Bayesian Estimation

Assume that δ, η, ζ, and ρ are R.Vs corresponding to the prior PDFs Gamma $(\delta; a_1, b_1)$, Gamma $(\eta; a_2, b_2)$, Gamma $(\zeta; a_3, b_3)$, respectively. Gamma $(\rho; a_4, b_4)$ follows, where a_i and b_i are positive constants and $i = 1, 2, 3, 4$. The posterior DF of $\delta, \eta, \zeta, \rho$ and the data under the gamma priors can take the following forms:

$$\begin{aligned} \pi_1(\delta) &= \frac{b_1^{a_1}}{\zeta(a_1)} \delta^{a_1 - 1} \exp[-b_1 \delta], \quad \delta, a_1, b_1 > 0, \\ \pi_2(\eta) &= \frac{b_2^{a_2}}{\zeta(a_2)} \eta^{a_2 - 1} \exp[-b_2 \eta], \quad \eta, a_2, b_2 > 0, \\ \pi_3(\zeta) &= \frac{b_3^{a_3}}{\zeta(a_3)} \zeta^{a_3 - 1} \exp[-b_3 \zeta], \quad \zeta, a_3, b_3 > 0, \\ \pi_4(\rho) &= \frac{b_4^{a_4}}{\zeta(a_4)} \rho^{a_4 - 1} \exp[-b_4 \rho], \quad \rho, a_4, b_4 > 0. \end{aligned} \quad (17)$$

Then, the posterior density of $\delta, \eta, \zeta, \rho$ and the data can be extracted as

$$\begin{aligned} \pi^*(\delta, \eta, \zeta, \rho \mid \mathbf{x}) &\propto \pi(\delta, \eta, \zeta, \rho) \\ \prod_{i=1}^{n} f(x_i; \delta, \eta, \zeta, \rho) &= J^{-1} \delta^{a_1 - 1} \eta^{a_2 - 1} \zeta_1^{a_3 - 1} \rho^{a_4 - 1} e^{-(b_1\delta + b_2\eta + b_3\zeta + b_4\rho) - \sum_{i=1}^{n} \delta x_i + \eta x_i^{\zeta} + \left(1 - e^{-\delta x_i - \eta x_i^{\zeta}}\right)^2} \\ &\cdot \prod_{i=1}^{n} \left(\delta + \eta\zeta x_i^{\zeta - 1}\right)\left(1 - e^{-\delta x_i - \eta x_i^{\zeta}}\right)\left(1 - \left(1 - e^{-\delta x_i - \eta x_i^{\zeta}}\right)^2\right)^{\rho - 1} \prod_{i=1}^{n}\left(1 + \rho - \left(1 - e^{-\delta x_i - \eta x_i^{\zeta}}\right)^2\right), \end{aligned} \quad (18)$$

where $x_i \geq 0, \delta, \eta, \zeta, \rho, a_i, b_i > 0$, $i = 1, 2, 3, 4$. And J is the normalizing constant.

5. MCMC Method

We use the Metropolis–Hastings (M-H) procedure as follows:

(1) Set initial values $\delta^{(0)}, \eta^{(0)}, \zeta^{(0)}$, and $\rho^{(0)}$. Then, simulate a sample of size n from NG-MW, next set $l = 1$.

(2) Simulate $\delta^{(*)}, \eta^{(*)}, \zeta^{(*)}$, and $\rho^{(*)}$ using the proposal distributions $N(\delta^{(l-1)}, V(\widehat{\delta}))$, $N(\eta^{(l-1)}, V(\widehat{\eta}))$, $N(\zeta^{(l-1)}, V(\widehat{\zeta}))$, and $N(\rho^{(l-1)}, V(\widehat{\rho}))$.

(3) Obtain the probability $r = \min((\pi^*(\delta^{(*)}, \eta^{(*)}, \zeta^{(*)}, \rho^{(*)})/\pi^*(\delta^{(l-1)}, \eta^{(l-1)}, \zeta^{(l-1)}, \rho^{(l-1)})), 1)$.

(4) Simulate U from Uniform (0, 1).

(5) If $U < r$, then $(\delta^{(l)}, \eta^{(l)}, \zeta^{(l)}, \rho^{(l)}) = (\delta^{(*)}, \eta^{(*)}, \zeta^{(*)}, \rho^{(*)})$. If $U \geq r$, then $(\delta^{(l-1)}, \eta^{(l-1)}, \zeta^{(l-1)}, \rho^{(l-1)}) = (\delta^{(*)}, \eta^{(*)}, \zeta^{(*)}, \rho^{(*)})$.

(6) Set $l = l + 1$.

(7) Iterate steps 2–6, M repetitions, and get $\delta^{(l)}, \eta^{(l)}, \zeta^{(l)}$ and $\rho^{(l)}$ for $l = 1, \ldots, M$.

Now, if we use the squared error loss function, given by $L_{SE}(\vartheta, \widehat{\vartheta}) = (\vartheta - \widehat{\vartheta})^2$, where $\widehat{\vartheta}$ is an estimate of the unknown parameter $\vartheta = \delta, \eta, \zeta$, and ρ against the loss function SE and

Table 2: Point and interval estimation of the parameters $\delta, \eta, \zeta, \rho$.

Parameter	Init.	a	B	Point ML	Point SE	Point LE1	Point LE2	Point GE	Interval ML	Interval HPD_S	Interval HPD_{LE1}	Interval HPD_{LE2}	Interval HPD_{GE}
	2.6	0.99	0.73	2.9078	2.6908	2.6936	2.6841	2.6853	0.209	2.594	2.5992	2.5854	2.587
									5.6066	2.945	2.9463	2.9426	2.9426
				0.3078	0.0908	0.0936	0.0841	0.0853	5.3975	0.351	0.3471	0.3571	0.3556
δ				1.8959	0.0301	0.0304	0.0295	0.0296					
									0.6359	2.631	2.6332	2.6194	2.6214
									5.1797	2.925	2.9255	2.9246	2.925
									4.5438	0.294	0.2923	0.3053	0.3035
	3.2	0.01	0.47	2.9078	3.1875	3.1908	3.1798	3.1823	0.426	2.853	2.8526	2.8525	2.8526
									5.3896	3.283	3.2869	3.2718	3.2764
				−0.2922	−0.0125	−0.0092	−0.0202	−0.0177	4.9636	0.43	0.4344	0.4193	0.4238
η				1.6033	0.029	0.0289	0.0292	0.0291					
									0.8185	2.881	2.8826	2.8788	2.879
									4.9971	3.245	3.2498	3.2331	3.2364
									4.1785	0.364	0.3672	0.3543	0.3574
	5.01	0.64	0.29	2.4463	5.0218	5.0254	5.0135	5.0182	0.0001	4.753	4.7584	4.7445	4.7455
									5.3299	5.263	5.2657	5.2582	5.2611
				−2.5636	0.0118	0.0154	0.0035	0.0082	5.3298	0.51	0.5072	0.5137	0.5156
ζ				2.1645	0.0296	0.0296	0.0297	0.0296					
									0.0188	4.788	4.7911	4.7821	4.7857
									4.8738	5.223	5.2264	5.2138	5.2192
									4.8551	0.435	0.4353	0.4317	0.4335
	3.7	0.26	0.52	3.2558	3.4274	3.4283	3.4255	3.4262	0.2639	3.308	3.3081	3.3081	3.3081
									6.2477	3.39	3.3902	3.3887	3.3891
				−0.4442	−0.2726	−0.2717	−0.2745	−0.2738	5.9838	0.082	0.0822	0.0807	0.081
ρ				2.3301	0.0798	0.0794	0.0807	0.0803					
									0.7371	3.312	3.3125	3.3124	3.3124
									5.7745	3.384	3.3846	3.3836	3.3841
									5.0373	0.072	0.0721	0.0712	0.0717

Point estimate: the first line represents estimate, the second line represents bias, and the third line represents ER. Interval estimate: 95% and 90% interval estimate, respectively. The first and second lines show the credible HPD interval and the corresponding width of the parameter, respectively.

is the posterior mean. Using the generated random samples from the Gibbs sampling procedure above and for N is the burn, then the Bayesian estimator of ϑ, say $\widehat{\vartheta}_{SE}$, can be obtained as

$$\widehat{\vartheta}_{SE} = E_{\vartheta}[\vartheta|\mathbf{x}] = \frac{1}{M-N}\sum_{l=N+1}^{M}\vartheta^{(l)}. \tag{19}$$

The second loss function is the LINEX loss function, given by

$$L_{LE}(\vartheta,\widehat{\vartheta}) = \exp[\varpi(\vartheta-\widehat{\vartheta})] - \varpi(\vartheta-\widehat{\vartheta}) - 1, \quad \rho \neq 0. \tag{20}$$

The approximate Bayes estimate of $\vartheta = \sigma, \delta, \zeta$, and ρ under LE loss function based on the Gibbs sampling technique, becomes

$$\widehat{\vartheta}_{LE} = \frac{-1}{\varpi}\log\left(E_{\vartheta}[\exp(-\varpi\vartheta)|\mathbf{x}]\right) = \frac{-1}{\varpi}\log\left(\frac{\sum_{l=N+1}^{M}\exp\left(-\varpi\vartheta^{(l)}\right)}{M-N}\right). \tag{21}$$

Finally, the general entropy (GE) loss function, given by

$$L_{GE}(\vartheta,\widehat{\vartheta}) = \left(\frac{\widehat{\vartheta}}{\vartheta}\right)^{\varepsilon} - \varepsilon\log\left(\frac{\widehat{\vartheta}}{\vartheta}\right) - 1. \tag{22}$$

The approximate Bayes estimate of the parameters, given by

$$\widehat{\vartheta}_{GE} = E_{\vartheta}\left([\vartheta^{-\varepsilon}|\mathbf{x}]\right)^{(-1/\varepsilon)} = \left(\frac{1}{M-N}\sum_{l=N+1}^{M}\left(\vartheta^{(l)}\right)^{-\varepsilon}\right)^{(-1/\varepsilon)}. \tag{23}$$

The MCMC HPD credible interval algorithm procedure is as follows:

(1) Sort $\delta^{(*)}, \eta^{(*)}, \zeta^{(*)}$, and $\rho^{(*)}$ in rising values.

(2) The lower bounds of δ, η, ζ, and ρ in the rank $(M-N) * (\varepsilon/2)$.

(3) The lower bounds of δ, η, ζ, and ρ in the rank $(M-N) * (1-(\varepsilon/2))$.

(4) Iterate the previous steps M times. Get the average value of the lower and upper bounds of δ, η, ζ, and ρ.

The first and second lines show the credible HPD interval and the corresponding width of the parameter, respectively.

Table 3: Point and interval estimation of the parameters $\delta, \eta, \zeta, \rho$ via the COVID-19 dataset.

Parameter	a	b	Point					Interval	
			ML	SE	LE1	LE2	GE	ML	HPD$_S$
δ	0.27	0.23	0.2738 0.0167	0.2317 $1.30E-09$	0.2316 $9.90E-31$	0.2316 $3.70E-32$	0.2316 $1.20E-32$	0.0167 0.5233 0.5066 0.0568 0.4832 0.4265	0.1212 0.2639 0.1427 0.4999 0.6933 0.1934
η	0.55	0.64	0.6387 0.0641	0.2497 $1.00E-04$	0.2497 $5.10E-05$	0.2497 $5.10E-05$	0.2496 0.0001	0.1438 1.1362 0.9925 0.2223 1.0577 0.8355	0.2247 0.2543 0.0296 0.2295 0.2522 0.0227
ζ	0.5	0.52	0.5243 0.0259	0.4457 $2.80E-32$	0.4457 0.0004	0.4455 0.0004	0.4449 0.0004	0.2046 0.8354 0.6309 0.2545 0.7855 0.5311	0.3705 0.4542 0.0837 0.389 0.4542 0.0652
ρ	0.18	0.52	0.5194 0.0998	0.4999 $2.80E-32$	0.4999 $2.70E-32$	0.4999 $1.20E-32$	0.4999 $2.70E-32$	0.0001 1.1391 1.139 0.0001 1.0412 1.0411	0.4999 0.7598 0.2599 0.4999 0.6933 0.1934

Point estimate: the first line represents estimate and the second line represents ER. Interval estimate: 95% and 90% interval estimate, respectively.

6. Numerical Calculations

First, we simulate $M = 1000$ samples of size $n = 50$ from the model NG-MW over initial parameter values $\delta^{(0)} = 2.6, \eta^{(0)} = 3.2, \zeta^{(0)} = 5.01$, and $\rho^{(0)} = 3.7$. In this simulation study, we empirically determine the biases and expected risks (ER) of the MLEs and Bayesian methods for the different parameter combinations of each sample. The point estimates of the parameters using the 200 burns MCMC methods are obtained. Two LINEX loss functions are used: $LE1$ when $\varpi = -0.3$ and $LE2$ when $\varpi = 0.7$. The biases and ERs are given respectively by

$$\begin{aligned} \operatorname{Bias}(\widehat{\vartheta}) &= \frac{1}{1000} \sum_{i=1}^{1000} \left(\widehat{\vartheta}_i - \vartheta\right), \\ \operatorname{ER}(\widehat{\vartheta}) &= \frac{1}{1000} \sum_{i=1}^{1000} \left(\widehat{\vartheta}_i - \vartheta\right)^2. \end{aligned} \tag{24}$$

Coverage probabilities (CPs) are also calculated for the 95% and 90% HPD credibility intervals. Simulation results are shown in Table 2 for parameters δ, η, ζ, and ρ.

Next, the COVID-19 dataset (see, [4]) is considered as an application of the NG-MW model and is given by 0.054, 0.064, 0.704, 0.816, 0.235, 0.976, 0.865, 0.364, 0.479, 0.568, 0.352, 0.978, 0.787, 0.976, 0.087, 0.548, 0.796, 0.458, 0.087, 0.437, 0.421, 1.978, 1.756, 2.089, 2.643, 2.869, 3.867, 3.890, 3.543, 3.079, 3.646, 3.348, 4.093, 4.092, 4.190, 4.237, 5.028, 5.083, 6.174, 6.743, 7.274, 7.058, 8.273, 9.324, 10.827, 11.282, 13.324, 14.278, 15.287, 16.978, 17.209, 19.092, 20.083. The expected real results are shown in Table 3 for the parameters δ, η, ζ, and ρ.

Table 4 compares the NG-MW distribution based on some recognition criteria, such as the Akaike information criterion (AIC), Bayesian information criterion (BIC), Hannan–Quinn information criterion (HQIC), and the consistent Akaike information criterion (CAIC). The goodness-of-fit results of the NG-MW model are compared with some other models, including Weibull, NG-Weibull (NG-W), and NG-exponential (NG-Exp) distributions.

Table 4: Relative quality of the NG-MW vs competing models.

Model	AIC	CAIC	BIC	HQIC
NG-W	273.0032	273.493	278.9141	275.2762
NG-MW	274.5728	275.4061	282.454	277.6035
NG-Exp	282.32	282.56	286.2606	283.8354
Weibull	321.4568	321.9466	327.3677	323.7298

7. Conclusion

In this paper, a four-parameter extension of the Weibull distribution, the new generalized modified Weibull distribution, is discussed in detail. Maximum likelihood and Bayesian estimation are used to estimate the model parameters. A simulation study was conducted to evaluate the performance of the new generalized modified Weibull distribution. The flexibility and usefulness of the proposed new generalized modified Weibull distribution is shown in the analysis of COVID-19 data. The new generalized modified Weibull model outperformed many other old models, as shown in the results in Table 4. The performance of the Bayesian estimates is more excellent than that of the corresponding ML estimators. The results indicate that the generalized Weibull model, as a special case of the new generalized modified Weibull model, provides a better fit than other competing models. We found that the proposed model provides a better characterization of COVID-19 events by analyzing daily death data. Therefore, it can be a perfect model for predicting future cases.

Data Availability

All the datasets used in this paper are available from the corresponding author upon request.

Conflicts of Interest

The authors declare that they have no conflicts of interest.

Acknowledgments

This study was funded by Researchers Supporting Project number (RSP2022R488), King Saud University, Riyadh, Saudi Arabia.

References

[1] M. Arfan, H. Alrabaiah, M. U. Rahman et al., "Investigation of fractal-fractional order model of COVID-19 in Pakistan under Atangana-Baleanu Caputo (ABC) derivative," *Results in Physics*, vol. 24, Article ID 104046, 2021.

[2] Y. Chen, J. Cheng, Y. Jiang, and K. Liu, "A time delay dynamical model for outbreak of 2019-nCoV and the parameter identication," *Journal of Inverse and Ill-Posed Problems*, vol. 28, no. 2, pp. 243–250, 2020.

[3] V. M. Corman, O. Landt, M. Kaiser et al., "Detection of 2019 novel coronavirus by real-time RT-PCR," *Euro Surveillance*, vol. 25, pp. 1–18, 2020.

[4] H. G Hong and Y Li, "Estimation of time-varying reproduction numbers underlying epidemiological processes: a new statistical tool for the COVID-19 pandemic," *PLoS One*, vol. 15, Article ID e0236464, 2020.

[5] D. Langemann, I. Nesteruk, and J. Prestin, "Comparison of mathematical models for the dynamics of the Chernivtsi children disease," *Mathematics and Computers in Simulation*, vol. 23, pp. 68–79, 2016.

[6] B. F Maier and D Brockmann, "Effective containment explains subexponential growth in recent confirmed COVID-19 cases in China," *Science (New York, N.Y.)*, vol. 368, pp. 742–746, 2020.

[7] I. Nesteruk, "Comparison of the coronavirus pandemic dynamics in Europe, USA and South Korea," *MedRxiv*, vol. 1, pp. 1–6, 2020.

[8] I. Nesteruk, "Simulations and predictions of COVID-19 pandemic with the use of SIR model," *Innovative Biosystems and Bioengineering*, vol. 4, pp. 110–121, 2020.

[9] I. Nesteruk, "Statistics-based predictions of coronavirus epidemic spreading in mainland China," *Innovative Biosystems and Bioengineering*, vol. 4, pp. 3–18, 2020.

[10] S. A. Sarkodie and P. A. Owusu, "Investigating the cases of novel coronavirus disease in China using dynamic statistical techniques," *Heliyon*, vol. 6, no. 4, pp. 1–5, 2020.

[11] K. Shah, M. Sher, H. Rabai'ah, A. Ahmadian, S. Salahshour, and B. A. Pansera, "Analytical and Qualitative Investigation of COVID-19 Mathematical Model under Fractional Differential Operator," *Mathematical Methods in the Applied Sciences*, 2021.

[12] L. Ying, A. A. Gayle, A. Wilder-Smith, and J. Rocklöv, "The reproductive number of COVID-19 is higher compared to SARS coronavirus," *Journal of Travel Medicine*, vol. 27, pp. 1–16, 2020.

[13] J. Zhao, Z. Ahmed, and Z. Almaspoor, "Modeling the COVID-19 pandemic dynamics in Iran and China," *Computers, Materials & Continua*, vol. 67, pp. 2111–2121, 2021.

[14] M. Zuo, S. K. Khosa, Z. Ahmad, and Z. Almaspoor, "Comparison of COVID-19 pandemic dynamics in Asian countries with statistical modeling," *Computational and Mathematical Methods in Medicine*, vol. 2020, pp. 1–16, Article ID 4296806, 2020.

[15] K. Dutta and J. Perry, "A Tale of Tails: An Empirical Analysis of Loss Distribution Models for Estimating Operational Risk Capital," *SSRN Electronic Journal*, 2006.

[16] Z. Ahmad, E. Mahmoudi, G. G. Hamedani, and O. Kharazmi, "New contribution towards families of distributions: properties, characterizations and an application to a heavy tailed data in the insurance sciences," *Journal of Taibah University for Science*, vol. 14, no. 1, pp. 359–382, 2020.

[17] Z. A. Ahmad, E. Mahmoudi, and E. Mahmoudi, "A family of loss distributions with an application to the vehicle insurance loss data," *Pakistan Journal of Statistics and Operation Research*, vol. 15, pp. 731–744, 2019.

[18] F. Jamal and M. Nasir, "Some new members of the TX family of distributions," *Al.Archives-Ouvertes.Fr*, vol. 17, 2019.

[19] A. Nasir, H. M. Yousof, F. Jamal, and M. C. Korkmaz, "The exponentiated Burr XII power series distribution: properties and applications," *Stat*, vol. 2, pp. 15–31, 2019.

[20] H. Al-Mofleh, "On generating a new family of distributions using the tangent function," *Pakistan Journal of Statistics and Operation Research*, vol. 14, no. 3, pp. 471–499, 2018.

[21] A. Z Afify, G. M Cordeiro, M. E Maed, M Alizadeh, H Al-Mofleh, and Z. M Nofal, "The generalized odd Lindley-G family: properties and applications," *Anais da Academia Brasileira de Ciencias*, vol. 91, Article ID e20180040, 2019.

[22] A. Z. Afify and M. Alizadeh, "The odd Dagum family of distributions: properties and applications," *Journal of Applied Probability and Statistics*, vol. 15, pp. 45–72, 2020.

[23] G. M. Cordeiro, A. Z. Afify, E. M. M. Ortega, A. K. Suzuki, and M. E. Mead, "The odd Lomax generator of distributions: properties, estimation and applications," *Journal of Computational and Applied Mathematics*, vol. 347, pp. 222–237, 2019.

[24] A. Alzaatreh, C. Lee, and F. Famoye, "A new method for generating families of continuous distributions," *Metron*, vol. 71, no. 1, pp. 63–79, 2013.

[25] A. M. Sarhan and M. Zaindin, "Modified Weibull distribution," *Applied Sciences*, vol. 11, pp. 123–136, 2009.